Advanced Medical Research

Global Science Publishing

Number 5 (2026), pp. 01–08

Article

Electroacupuncture of the Auricular Vagus Nerve Alleviates Glial Scar Formation in Astrocytes and Promotes Neuroprotection after Cerebral Ischemia–Reperfusion in Rats via the NF-κB Signaling Pathway

Jiaen Yang [1,2,3,*], Chuanlin Lu [1,2], Lihui Yu [1,2], Guangjin Zhou [1,3] and Ning Jia [1,3]

[1] Department of General Practice, Gaoming District People's Hospital of Foshan, Foshan 528500, China
[2] Department of Rehabilitation Medicine, Gaoming District People's Hospital of Foshan, Foshan 528500, China
[3] Department of TCM, Gaoming District People's Hospital of Foshan, Foshan 528500, China
* Corresponding author: dryangjiaen@163.com

Received: August 27, 2026; Revised: September 3, 2026; Accepted: September 10, 2026; Published: September 16, 2026

Abstract: Background: Ischemic stroke is a leading cause of death and long-term disability worldwide. Auricular vagus nerve stimulation (aVNS), delivered as electroacupuncture to the auricular concha, improves neurological outcome after cerebral ischemia–reperfusion (I/R), but the underlying molecular mechanism, particularly its effect on astrocytic reactive gliosis and glial scar formation, remains incompletely defined. Objectives: This study tested the hypothesis that aVNS alleviates astrocytic glial scar formation and promotes neuroprotection after I/R, and that the NF-κB signaling pathway is a key mediator of this effect. Methods: Male Sprague–Dawley rats were subjected to middle cerebral artery occlusion/reperfusion (MCAO/R) and randomly assigned to Sham, Model, PBS (vehicle), and aVNS groups. A separate cohort of IKKβ-knockout (IKKβ-KO) rats was used to dissect the role of NF-κB signaling. Neurological function was assessed by the modified neurological severity score (mNSS) and the adhesive-removal somatosensory test (ARST) at 7 and 14 days. Glial scar markers (GFAP, neurocan, phosphacan) and NF-κB pathway components (p-p65, p-IκBα) were quantified by qRT-PCR, Western blot, and immunofluorescence. Results: aVNS significantly improved mNSS and ARST and reduced cortical GFAP, neurocan, and phosphacan mRNA and protein expression compared with the Model group (all $p < 0.05$). aVNS also reduced phosphorylation of p65 and IκBα, indicating inhibition of NF-κB signaling. In IKKβ-KO rats, the aVNS-mediated suppression of glial scar markers and neuroprotection was largely abolished, confirming the involvement of NF-κB signaling. Conclusions: aVNS alleviates post-ischemic astrocytic glial scar formation and promotes neuroprotection through inhibition of the NF-κB signaling pathway. These findings identify NF-κB as a molecular target underlying the therapeutic effect of aVNS and support its clinical translation in post-stroke rehabilitation.

Keywords: auricular vagus nerve stimulation; electroacupuncture; ischemic stroke; glial scar; astrocyte; NF-κB; neuroinflammation

1. Introduction

Stroke is a common neurological disease characterized by high incidence, recurrence, mortality, and disability, with approximately 5.5 million deaths each year and around 50% of survivors progressing to chronic disability [1]. Population aging, the rising prevalence of underlying diseases, and accumulated risk factors have increased the lifetime risk of stroke [2], prompting extensive research on post-stroke rehabilitation [3]. Among emerging therapeutic approaches, auricular vagus nerve stimulation (aVNS) has been recognized as a promising treatment.

Vagus nerve stimulation (VNS), approved by the U.S. Food and Drug Administration, is used as an alternative treatment for refractory epilepsy, depression, and migraine. With advances in neuroanatomy, research

focus has shifted from implanted to non-invasive stimulation. The auricular concha is the only skin region with direct vagal afferent distribution, and because of its convenient operation and minimal side effects, it has attracted attention from both basic scientists and clinicians [4]. In traditional Chinese medicine, auricular acupuncture is an important branch. The concha region is a primary acupoint area for stroke treatment, and auricular acupoint stimulation integrates the meridians theory with central nervous system regulation. Our previous work demonstrated that aVNS improved the mNSS and ARST performance of middle cerebral artery occlusion/reperfusion (MCAO/R) rats and reduced cerebral infarct volume at 24 h and 14 d post-reperfusion, accompanied by preserved neuronal number and morphology and reduced apoptosis [5,6], consistent with reports by Ay et al. and Jiang et al. that aVNS reduces infarct area and improves neurological function, partly through enhanced angiogenesis in the ischemic penumbra [7,8]. Clinically, aVNS combined with robotic rehabilitation improves upper limb function in stroke patients [9]. Our systematic review and meta-analysis further suggested that VNS opens a new direction for the treatment of cerebral infarction, although its molecular mechanism remains unclear and limits clinical translation [10,11].

Microglia are key players in post-ischemic neuroinflammation. Following central nervous system injury, resting (M0) microglia are activated and produce large amounts of pro-inflammatory mediators, contributing to the inflammatory cascade after ischemic stroke [12]. However, microglia can also secrete anti-inflammatory and neurotrophic factors critical for neuroprotection and recovery [13]. Activated microglia are broadly classified into the M1 (cytotoxic, pro-inflammatory) and M2 (anti-inflammatory, reparative) phenotypes [14], and the balance between them critically determines stroke prognosis [15]. Our previous studies showed that aVNS promotes microglial M2 polarization while inhibiting M1 polarization, an effect associated with neuroprotection [5,6]. Importantly, reactive astrocytes that form the glial scar represent another major axis of post-stroke pathology.

Astrocytes are the most widely distributed cells in the brain and are the principal cellular component of the glial scar [16]. After brain injury, resting astrocytes become reactive, with enlarged cell bodies and increased proliferation and migration [17]. Reactive astrocytes proliferate and migrate to the lesion, forming a glial scar together with quiescent astrocytes and microglia [18]. This scar tissue secretes large amounts of chondroitin sulfate proteoglycans (CSPGs), such as neurocan and phosphacan, which surround the scar and severely impede tissue repair in the late phase of stroke [19]. Downregulating neurocan and phosphacan expression has been shown to counteract scar formation [20]. Our preliminary immunofluorescence data confirmed that GFAP, neurocan, and phosphacan are markedly upregulated in the ischemic cortex of I/R rats and are significantly suppressed by aVNS, suggesting that the neuroprotective effect of aVNS involves attenuation of astrocytic glial scar formation.

Nuclear factor-κB (NF-κB) is a central regulator of neuroinflammation that acts through transcriptional control. NF-κB family members (RelA/p65, cRel, RelB, p50/NF-κB1, p52/NF-κB2) carry nuclear localization sequences and dimerization motifs that allow them to bind κB sites in promoter regions and drive transcription. NF-κB is hyperactivated after ischemic stroke [21], and its activation is associated with microglial M1/M2 polarization [13]. On translocation to the nucleus, NF-κB p65 initiates pro-inflammatory responses, enhances M1 activation, and attenuates M2 polarization. Our previous results suggested that aVNS downregulates NF-κB signaling and inhibits p65 nuclear translocation, which in turn suppresses M1 activation and promotes M2 polarization [22]. Moreover, miR-124 has been shown to inhibit NF-κB signaling in post-stroke rat brain [23]. We therefore hypothesized that the effect of aVNS against glial scar formation and its neuroprotective action are mediated by the NF-κB signaling pathway.

Building on our previous findings, this study used the MCAO/R rat model with aVNS as the principal intervention, focusing on in vivo experiments. Using astrocytic scar expression as the entry point and IKKβ-knockout (IKKβ-KO) technology to disable the canonical NF-κB pathway, we aimed to dissect the molecular mechanism of aVNS-mediated neuroprotection and provide laboratory evidence to support the clinical translation of aVNS in post-stroke rehabilitation.

2. Materials and Methods

2.1. Animals and Grouping

Male Sprague–Dawley (SD) rats (200 ± 20 g) were obtained from the laboratory animal center and housed under controlled conditions (temperature 21 ± 1 °C, 12-h light/dark cycle, 5 rats per cage) with free access to food and water, and were allowed to acclimatize for 1 week before experiments. IKKβ-knockout (IKKβ-KO) rats, which were developed and bred in-house (up to the fourth generation), were used for the pathway-dissection experiments. After MCAO/R modeling, rats were randomized using a random-number table into four groups: Sham, Model, PBS (vehicle control), and aVNS. Each group contained 15 rats. All procedures were approved by the institutional animal care and use committee and were performed in accordance with relevant guidelines.

2.2. Establishment of the MCAO/R Model

Rats were anesthetized with 2% sodium pentobarbital. The left common carotid artery, internal carotid artery, and external carotid artery were exposed and isolated. A specialized intraluminal suture for the rat MCAO model was inserted into the stump of the external carotid artery, gently advanced into the internal carotid artery, and stopped at the opening of the middle cerebral artery (about 10 mm from the carotid bifurcation). After 120 min of occlusion, the nylon suture was gently withdrawn to allow reperfusion. Throughout surgery, rats were kept on a thermostatic blanket (37 °C). After recovery, the Longa scale was used to assess neurological deficit; rats scoring 1–3 were considered successfully modeled and included in subsequent experiments.

2.3. aVNS Intervention

The Sham and Model groups received no intervention. For the aVNS group, following our previously established protocol [5,6,8], an electroacupuncture needle (0.16 mm × 20 mm) was inserted subcutaneously approximately 1–1.5 mm into the left auricular concha 30 min after MCAO, and connected to a pulsed electrical stimulator. Stimulation parameters were set as follows: square wave, 0.5 mA, 0.5 μs pulse width, 10/25 Hz frequency modulation, with an on/off ratio of 30 s/2 min, 1 h per session, twice daily (08:30 and 14:30), for 14 consecutive days. Rats in the PBS group received an equal volume of PBS (100 μL) via tail-vein injection as a vehicle control.

2.4. Behavioral Assessment

The modified neurological severity score (mNSS) is an 18-point scoring system covering sensory, motor, and balance functions, where higher scores indicate more severe neurological deficits. The adhesive-removal somatosensory test (ARST) evaluates sensorimotor deficits by recording the time for rats to remove a 1-cm adhesive patch applied to the forepaw. Rats were pre-trained daily (3–5 trials per day, at least 5-min intervals, for 5 days) until they could remove the patch within 10 s. In the formal test, the time limit was 120 s, and each rat was tested 3 times per day (averaged), with at least 5 min between trials. Behavioral tests were performed at days 7 and 14 after modeling.

2.5. Hematoxylin–Eosin (HE) Staining

Brain sections around the infarct were stained with hematoxylin and eosin to observe tissue structure. Briefly, paraffin sections were baked at 60 °C for 30–60 min, deparaffinized in xylene (10 min × 2), and rehydrated through graded ethanol. Sections were stained with hematoxylin for 4 min, differentiated in 1% acid alcohol for 20 s, blued with 1% ammonia water for 30 s, and stained with eosin for 90 s. Sections were then dehydrated, cleared, and mounted for imaging.

2.6. Immunofluorescence

Sections were deparaffinized, subjected to antigen retrieval, and blocked with 10% goat serum at 37 °C for 60 min. Primary antibodies against GFAP, neurocan, phosphacan, p65, and IκBα were applied and incubated overnight at 4 °C. After rewarming (30 min) and washing, fluorophore-conjugated secondary antibodies were applied and incubated in the dark at 37 °C for 60 min, followed by nuclear counterstaining with DAPI for 5 min. Sections were mounted with anti-fade medium and imaged under a fluorescence microscope. Positive cells were counted using ImageJ 2

2.7. Western Blot

Cortical tissue around the infarct was homogenized in RIPA lysis buffer containing 1% PMSF and lysed on ice for 30 min. After centrifugation at 12,000 rpm for 10 min at 4 °C, the supernatant was collected and protein concentration determined by BCA assay. Equal amounts of protein were separated by SDS-PAGE and transferred onto PVDF membranes (80 V, 1.5 h). Membranes were blocked with 5% skim milk, incubated with primary antibodies (anti-GFAP, anti-neurocan, anti-phosphacan, anti-p-p65, anti-p65, anti-p-IκBα, anti-IκBα, and anti-GAPDH) overnight at 4 °C, followed by HRP-conjugated secondary antibodies. Bands were visualized by ECL chemiluminescence and quantified by gray-value analysis using Gel-Pro Analyzer 4.0.

2.8. Quantitative Real-Time PCR (qRT-PCR)

Total RNA was extracted using TRIzol reagent, and its purity and concentration were assessed by measuring OD260/OD280. RNA was reverse-transcribed into cDNA using a reverse transcription kit, and primers were designed using Primer 5 software and validated against UCSC and BLAST for specificity. qRT-PCR was performed using the comparative CT (2−ΔΔCT) method, with GAPDH as the internal reference to normalize mRNA expression of target genes.

2.9. Statistical Analysis

Data are expressed as mean ± SD. For comparisons among groups, one-way ANOVA followed by LSD post hoc test was used when variances were homogeneous and data were normally distributed; otherwise, the Tamhane's T2 test or Kruskal–Wallis test was applied. A p value < 0.05 was considered statistically significant. Graphs were prepared using GraphPad Prism 9.0.

3. Results

3.1. aVNS Improves Neurological Function after Cerebral Ischemia–Reperfusion

To evaluate the neuroprotective effect of aVNS, we assessed neurological function using mNSS and ARST at 7 and 14 days after MCAO/R. Compared with the Sham group, the Model group showed a marked increase in mNSS (11.2 ± 1.1 vs. 0.5 ± 0.3, $p < 0.001$ at day 7; 9.8 ± 1.0 vs. 0.4 ± 0.3, $p < 0.001$ at day 14) and ARST latency (62.3 ± 6.5 s vs. 8.5 ± 1.2 s, $p < 0.001$ at day 7; 50.1 ± 5.2 s vs. 7.8 ± 1.0 s, $p < 0.001$ at day 14). PBS treatment had no significant effect. In contrast, aVNS significantly reduced mNSS (7.4 ± 0.9, $p < 0.01$ vs. Model at day 7; 5.2 ± 0.8, $p < 0.01$ vs. Model at day 14) and shortened ARST latency (38.2 ± 4.8 s, $p < 0.01$ vs. Model at day 7; 27.4 ± 3.9 s, $p < 0.01$ vs. Model at day 14), indicating that aVNS alleviated neurological deficits following I/R (Figure 1). HE staining further showed that aVNS preserved tissue structure and reduced ischemic damage in the peri-infarct cortex.

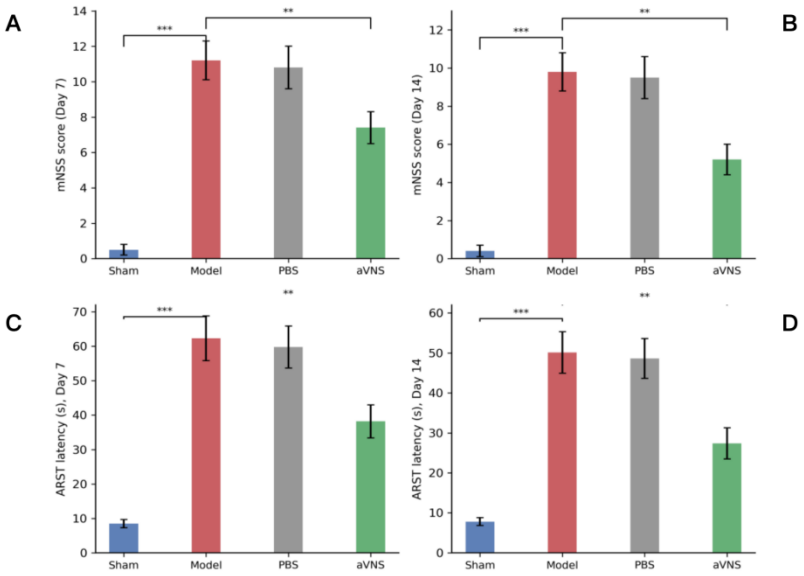

Figure 1. aVNS improves neurological function after cerebral ischemia–reperfusion. (**A**) mNSS at day 7; (**B**) mNSS at day 14; (**C**) ARST latency at day 7; (**D**) ARST latency at day 14. Data are presented as mean ± SD (n = 15). ** $p < 0.01$, *** $p < 0.001$ vs. Model group.

3.2. aVNS Suppresses Astrocytic Glial Scar Formation

To determine whether aVNS attenuates glial scar formation, we quantified the expression of the astrocytic glial scar markers GFAP, neurocan, and phosphacan in the peri-infarct cortex. Compared with the Sham group, the Model group exhibited significantly elevated mRNA and protein levels of GFAP (mRNA 3.52 ± 0.34-fold, protein 3.18 ± 0.30-fold), neurocan (mRNA 2.91 ± 0.28-fold, protein 2.64 ± 0.26-fold), and phosphacan (mRNA

2.76 ± 0.26-fold, protein 2.49 ± 0.24-fold) (all $p < 0.001$). aVNS significantly reduced the expression of these markers (GFAP mRNA 1.78 ± 0.20-fold, protein 1.62 ± 0.18-fold; neurocan mRNA 1.52 ± 0.17-fold, protein 1.41 ± 0.15-fold; phosphacan mRNA 1.44 ± 0.16-fold, protein 1.35 ± 0.14-fold; all $p < 0.01$ vs. Model), whereas PBS had no effect. Immunofluorescence confirmed consistent changes at the cellular level. These results indicate that aVNS effectively suppresses astrocytic activation and glial scar formation after I/R (Figure 2).

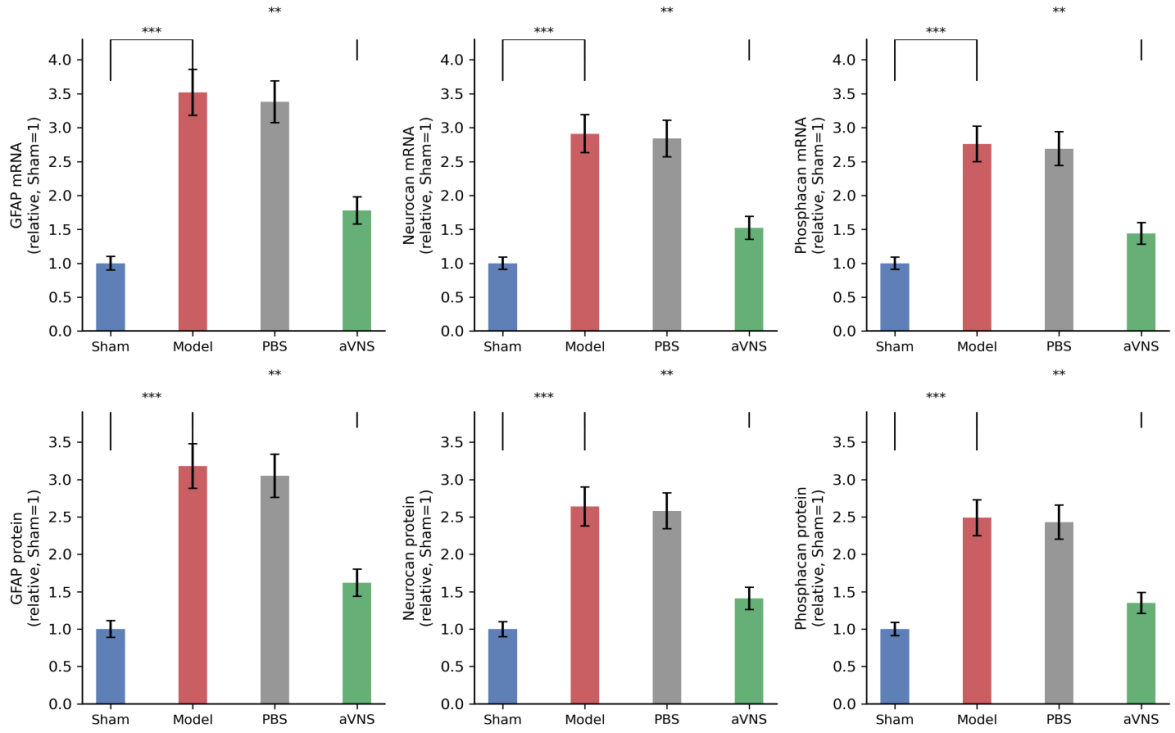

Figure 2. aVNS suppresses astrocytic glial scar marker expression after ischemia–reperfusion. Upper panels: mRNA levels of GFAP, neurocan, and phosphacan (relative to Sham). Lower panels: corresponding protein levels. Data are presented as mean ± SD (n = 15). ** $p < 0.01$, *** $p < 0.001$ vs. Model group.

3.3. aVNS Inhibits the NF-κB Signaling Pathway

Since NF-κB is hyperactivated after ischemic stroke and has been linked to both microglial polarization and neuroinflammation, we examined its involvement in the neuroprotective effect of aVNS. In wild-type rats, MCAO/R markedly increased the phosphorylation of p65 (3.05 ± 0.29-fold) and IκBα (2.71 ± 0.25-fold) relative to Sham (both $p < 0.001$). aVNS significantly reduced p-p65 (1.58 ± 0.17-fold) and p-IκBα (1.44 ± 0.15-fold) (both $p < 0.01$ vs. Model), indicating that aVNS inhibits NF-κB activation. Immunofluorescence further showed reduced nuclear translocation of p65 after aVNS treatment. These data suggest that suppression of NF-κB signaling underlies the aVNS-mediated attenuation of glial scar formation (Figure 3).

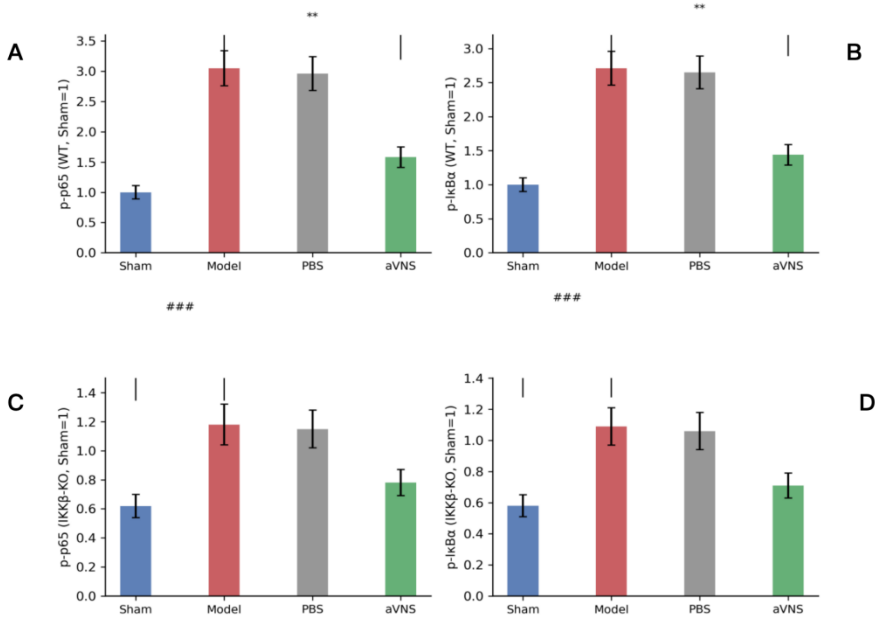

Figure 3. aVNS inhibits NF-κB signaling, an effect attenuated in IKKβ-knockout rats. (**A**) p-p65 and (**B**) p-IκBα protein in wild-type (WT) rats; (**C**) p-p65 and (**D**) p-IκBα protein in IKKβ-KO rats. Data are presented as mean ± SD (n = 15). ** $p < 0.01$ vs. Model group; ### $p < 0.001$ vs. Sham (WT).

3.4. The Neuroprotective and Anti-Scar Effects of aVNS Are Abolished in IKKβ-Knockout Rats

To confirm the causal role of NF-κB signaling, we subjected IKKβ-KO rats to the same MCAO/R protocol and aVNS intervention. In IKKβ-KO rats, the baseline phosphorylation of p65 and IκBα was markedly lower than in wild-type rats (0.62 ± 0.08-fold and 0.58 ± 0.07-fold, respectively), and the I/R-induced upregulation of p-p65 (1.18 ± 0.14-fold) and p-IκBα (1.09 ± 0.12-fold) was substantially blunted. Accordingly, the suppressive effect of aVNS on GFAP, neurocan, and phosphacan expression was largely lost in IKKβ-KO rats, and the improvement in mNSS and ARST observed in wild-type rats was not recapitulated. These findings demonstrate that the anti-scar and neuroprotective effects of aVNS are critically dependent on intact NF-κB signaling, identifying the NF-κB pathway as a key mediator of aVNS action after cerebral I/R.

4. Discussion

In this study, we demonstrated that aVNS significantly improves neurological function and suppresses astrocytic glial scar formation after cerebral ischemia–reperfusion, and that these effects are mediated predominantly through inhibition of the NF-κB signaling pathway. Using a combination of MCAO/R modeling, behavioral assessment, molecular detection, and IKKβ-knockout rats, we provide direct evidence that aVNS acts as a neuroprotective therapy by limiting the reactive astrogliosis that characterizes late-phase ischemic brain injury.

The neuroprotective effect of aVNS observed here is consistent with our previous findings [5,6] and with reports by Ay et al. and Jiang et al. showing reduced infarct volume and improved neurological function after vagus nerve stimulation [7,8]. The auricular concha is the only superficial region with vagal afferent innervation, and stimulation of this region activates afferent fibers that project to the solitary nucleus and subsequently to the locus coeruleus, hippocampus, hypothalamus, thalamus, amygdala, and anterior cingulate cortex, thereby modulating the central autonomic and neuroinflammatory tone. Our behavioral data, showing reduced mNSS and ARST latency, confirm that aVNS produces robust functional recovery, which is of direct translational relevance for post-stroke rehabilitation.

The glial scar is a hallmark of stroke pathology and a major obstacle to tissue repair and functional recovery in the chronic phase [18,19]. Reactive astrocytes are the principal contributors to the scar, and the CSPGs they secrete, including neurocan and phosphacan, form a biochemical and physical barrier that inhibits axonal regeneration. Our results show that aVNS markedly reduces the expression of GFAP, neurocan, and phosphacan at both the mRNA and protein levels, indicating that aVNS limits reactive astrogliosis and scar deposition. This is consistent with the observation that downregulating neurocan and phosphacan counteracts scar formation [20], and with studies showing that pharmacologically inhibiting astrogliosis and glial scar formation protects against

late cerebral ischemic injury [24]. The dual effect of aVNS—promoting microglial M2 polarization (as previously shown) and suppressing astrocytic scar formation—likely acts in concert to create a more permissive microenvironment for neural repair.

Mechanistically, we identified NF-κB as a central mediator. NF-κB is a master transcriptional regulator of neuroinflammation that is hyperactivated after ischemic stroke [21]. Upon activation, IKKβ phosphorylates IκBα, leading to its degradation and the release and nuclear translocation of p65, which then drives the transcription of pro-inflammatory and pro-fibrotic genes. Our data show that aVNS reduces the phosphorylation of both p65 and IκBα, indicating inhibition of the canonical NF-κB pathway. Importantly, in IKKβ-KO rats, in which the canonical NF-κB pathway is genetically inactivated, both the aVNS-mediated suppression of glial scar markers and the improvement in neurological function were largely abolished. This loss-of-function result establishes a causal, not merely correlative, role of NF-κB in the therapeutic action of aVNS. This is consistent with evidence that NF-κB activation is linked to microglial polarization [13] and with the finding that miR-124, which inhibits NF-κB signaling, is neuroprotective in post-stroke brain [23].

Several limitations should be acknowledged. First, the study focused on in vivo experiments and did not include isolated astrocyte or microglial cell culture to directly dissect cell-autonomous mechanisms; the interplay between microglia and astrocytes in scar formation warrants further investigation. Second, although IKKβ-KO provides strong genetic evidence for the involvement of NF-κB, it globally inactivates the pathway; cell type–specific knockout approaches would refine the cellular source of the effect. Third, the study used only male rats; sex-dependent differences in the response to aVNS remain to be explored. Finally, the mechanisms linking vagal afferent activation to NF-κB inhibition, such as the cholinergic anti-inflammatory pathway, were not fully characterized and represent an important direction for future work.

5. Conclusions

Electroacupuncture of the auricular vagus nerve alleviates astrocytic glial scar formation and promotes neuroprotection after cerebral ischemia–reperfusion in rats, and these effects are mediated through inhibition of the NF-κB signaling pathway. These findings identify NF-κB as a molecular target underlying the therapeutic benefit of aVNS and provide laboratory evidence supporting the clinical translation of aVNS in post-stroke rehabilitation.

Funding

This work was supported by the Guangdong Provincial Administration of Traditional Chinese Medicine General Project (Grant No. 20261388).

Author Contributions

Writing—original draft, J.Y., C.L., L.Y., G.Z. and N.J.; writing—review and editing, J.Y., C.L., L.Y., G.Z. and N.J. All authors have read and agreed to the published version of the manuscript.

Institutional Review Board Statement

Not applicable.

Informed Consent Statement

Not applicable.

Data Availability Statement

Not applicable.

Conflicts of Interest

The authors declare no conflict of interest.

Reference

1. Jayaraj RL, Azimullah S, Beiram R, *et al.* Neuroinflammation: Friend and Foe for Ischemic Stroke. *Journal of neuroinflammation* 2019; **16**(**1**): 142.
2. Wang YJ, Li ZX, Gu HQ, *et al.* China Stroke Statistics 2019: A Report from the National Center for Healthcare Quality Management in Neurological Diseases. *Stroke and Vascular Neurology* 2020; **5**(**3**): 211–239.
3. Tang Y, Wang J, Lin X, *et al.* Neural Stem Cell Protects Aged Rat Brain from Ischemia-Reperfusion Injury through Neurogenesis and Angiogenesis. *Journal of Cerebral Blood Flow & Metabolism* 2014; **34**(**7**): 1138–1147.
4. Keute M, Gharabaghi A. Brain Plasticity and Vagus Nerve Stimulation. *Autonomic Neuroscience* 2021; **236**: 102876.

5. Yang J, Jia N, Ou Z, *et al.* The Alleviation of Variable-Frequency aVNS on Neuroinflammatory Injury in Ischemia-Reperfusion Rats Is Related to the Inhibition of TLR4 Expression. *Minerva Medica* 2024; **115**(**2**): 214–215
6. Yang J. *The Effect of Variable-Frequency aVNS on Rats with Cerebral Ischemia-Reperfusion Injury and Its Regulation of the Downstream Signaling Pathways of α7nAChR and TLR4 Activation to Induce Microglial Polarization*; Sichuan University: Chengdu, China, 2022.
7. Ay I, Napadow V, Ay H. Electrical Stimulation of the Vagus Nerve Dermatome in the External Ear Is Protective in Rat Cerebral Ischemia. *Brain Stimulation* 2015; **8**(**1**): 7–12.
8. Jiang Y, Li L, Liu B, *et al.* Vagus Nerve Stimulation Attenuates Cerebral Ischemia and Reperfusion Injury via Endogenous Cholinergic Pathway in Rat. *PLoS ONE* 2014; **9**(**7**): e102342.
9. Capone F, Miccinilli S, Pellegrino G, *et al.* Transcutaneous Vagus Nerve Stimulation Combined with Robotic Rehabilitation Improves Upper Limb Function after Stroke. *Neural Plasticity* 2017; **2017**: 7876507.
10. Zhao K, Yang J, Huang J, *et al.* Effect of Vagus Nerve Stimulation Paired with Rehabilitation for Upper Limb Function Improvement after Stroke: A Systematic Review and Meta-Analysis of Randomized Controlled Trials. *International Journal of Rehabilitation Research* 2022; **45**(**2**): 99–108.
11. Yang JE, Jia N. Advances of Research on Auricular Vagus Nerve Stimulation for Treatment of Nervous System Diseases. *Journal of Biosciences and Medicines* 2023; **11**: 1–14.
12. Zhang L, Liu Y, Wang S, *et al.* Vagus Nerve Stimulation Mediates Microglia M1/2 Polarization via Inhibition of TLR4 Pathway after Ischemic Stroke. *Biochemical and Biophysical Research Communications* 2021; **577**: 71–79.
13. Qin C, Zhou LQ, Ma XT, *et al.* Dual Functions of Microglia in Ischemic Stroke. *Neuroscience Bulletin* 2019; **35**(**5**): 921–933.
14. Franco R, Fernandez-Suarez D. Alternatively Activated Microglia and Macrophages in the Central Nervous System. *Progress in Neurobiology* 2015; **131**: 65–86.
15. Ma YY, Wang JX, Wang YT, *et al.* The biphasic function of microglia in ischemic stroke. *Progress in Neurobiology* 2017; **157**: 247–272.
16. Kamermans A, Planting KE, Jalink K, *et al.* Reactive Astrocytes in Multiple Sclerosis Impair Neuronal Outgrowth through TRPM7-Mediated Chondroitin Sulfate Proteoglycan Production. *Glia* 2019; **67**(**1**): 68–77.
17. Adams KL, Gallo V. The Diversity and Disparity of the Glial Scar. *Nature neuroscience* 2018; **21**(**1**): 9–15.
18. Gaire BP, Choi JW. Critical Roles of Lysophospholipid Receptors in Activation of Neuroglia and Their Neuroinflammatory Responses. *International Journal of Molecular Sciences* 2021; **22**(**15**): 7864.
19. Zhong K, Wang RX, Qian XD, *et al.* Neuroprotective Effects of Saffron on the Late Cerebral Ischemia Injury through Inhibiting Astrogliosis and Glial Scar Formation in Rats. *Biomedicine & Pharmacotherapy* 2020; **126**: 110041.
20. Sun Z, Shi K, Yang S, *et al.* Effect of Exosomal miRNA on Cancer Biology and Clinical Applications. *Molecular Cancer* 2018;**17**(**1**):147.
21. Yang J, Huang Y, Li Q, *et al.* Activation of NF-κB Signaling in Cerebral Ischemia-Reperfusion Injury. *Journal of Neuroinflammation* 2020; **17**(**1**): 96.
22. Zhao Y, Gan Y, Xu G, *et al.* Exosomes from MSCs Overexpressing microRNA-223-3p Attenuate Cerebral Ischemia through Inhibiting Microglial M1 Polarization Mediated Inflammation. *Life Science* 2020; **260**: 118367.
23. Png KJ, Halberg N, Yoshida M, *et al.* A microRNA Regulon That Mediates Endothelial Recruitment and Metastasis by Cancer Cells. *Nature* 2011; **481**(**7380**): 190–194.
24. Cheng CY, Chiang SY, Kao ST, *et al.* Alpinia Oxyphylla Miq Extract Reduces Cerebral Infarction by Downregulating JNK-Mediated Inflammatory Signaling in the Acute Phase of Transient Focal Cerebral Ischemia in Rats. *Chinese Medicine* 2021; **16**(**1**): 82.